NATIONAL AERONAUTICS AND SPACE ADMINISTRATION

Technical Memorandum 33-793

Large-Payload Earth-Orbit Transportation With Electric Propulsion

JET PROPULSION LABORATORY
CALIFORNIA INSTITUTE OF TECHNOLOGY
PASADENA, CALIFORNIA

September 15, 1976

PREFACE

The work described in this report was performed by the Propulsion Division of the Jet Propulsion Laboratory.

CONTENTS

TABLES

FIGURES

ABSTRACT

Economical unmanned Earth-orbit transportation for large payloads is evaluated. The high exhaust velocity achievable with electric propulsion is attractive because it will minimize the propellant that must be carried to low Earth orbit. Propellant transport is a principal cost item. Electric propulsion subsystems utilizing advanced ion thrusters are compared to MPD thrust subsystems. For very large payloads, a Large Lift Vehicle is needed to low Earth orbit, and argon propellant is required for electric propulsion. Under these circumstances, this study shows the MPD thruster to be desirable over the ion thruster for Earth-orbit transportation. Both solar-electric and nuclear-electric power supplies were considered.

I. INTRODUCTION

Studies (Refs. 1 and 2) indicate a growing need for large payloads in Earth orbit during the next 25 years. However, transportation that is economically attractive to deliver these payloads must yet be developed. This report considers the desirability of electric propulsion as well as chemical propulsion to meet Earth-orbit transportation requirements. Of basic concern is the delivery of payload and propellant to low Earth orbit (LEO) and subsequent transport to geosynchronous Earth orbit (GEO).

The main advantage of electric propulsion is that its high exhaust velocity minimizes the amount of propellant in LEO. This reflects into a major saving in launch cost. In addition, if the payload can be assembled in LEO and has large onboard power, the electric propulsion can utilize the onboard power to carry the system to GEO. Subsequent to arrival in GEO, the electric thrust subsystems can be utilized for attitude control and station keeping (at a much-reduced power level).

Assembly of the large payload in GEO would require separately powered electric propulsion for low-thrust cargo transport. Personnel transport to GEO for the assembly job requires high-thrust chemical propulsion for rapid transport. The low-thrust electric vehicles must be capable of multiple round trips through the Van Allen radiation belts (and particularly the proton belts). Such a vehicle may also be able to serve as a teleoperator at GEO to aid in deployment of payloads. In all probability, assembly in GEO will require larger transportation cost for crew and special equipment than will assembly in LEO.

Transport cost for large payloads may also be reduced by developing larger, unmanned launch vehicles. The anticipated minimum Shuttle cost to LEO is of the order of $300/kg. This can be further reduced to about $50/kg by an appropriate large lift vehicle (LLV). This can have a major impact on future economic desirability of large orbital payloads. A number of different concepts of LLV have been proposed (Ref. 2). For the studies below, we will simply assume the availability of LLV as well as adequate payload mass capability and cargo bay volume to handle all requirements to LEO at $50/kg.

The cargo orbit transfer vehicle (COTV) will be optimized on the basis of total transportation system cost. Because of this, it is more important to define scaling factors over a range of system mass than to establish point designs. A certain amount of arbitrariness is therefore allowable in the selection of hardware size.

The hardware chosen is considered only as an order-of-magnitude estimate of future needs and serves only to establish the parameters of performance and cost. We shall, for instance, assume an orbital payload power level of 4 GWe, assembled either in LEO or GEO. Mass of this module will be considered at 5, 10, and 15 kg/kWe. Several of these may be assembled in space annually. First-order comparisons of COTV options are to be made and a baseline candidate considered for more-detailed optimization, both for LEO and GEO assembly.

II. ELECTRIC THRUST SUBSYSTEM TECHNOLOGY

There are four types of electric thrusters available for COTV propulsion operation: the resistojet, arc jet, magnetoplasmadynamic (MPD) accelerator, and ion accelerator. Of these, the arc jet and MPD thruster are considered as variations of the same plasma device and will both be categorized under the broad heading of MPD thruster. The resistojet has a relatively low exhaust velocity (<8 km/s), and will not be considered in this report. Its potential availability will continue to be studied, but it does not at this time indicate a clear advantage over other alternatives.

In this section, the MPD thruster is estimated to have a constant 50% efficiency of converting electrical power to thrust, over a range of exhaust velocity between 10 and 50 km/s (Refs. 2, 3). The ion thruster operating on argon is constrained to an exhaust velocity above 50 km/s. According to a preliminary evaluation by LeRC, this lower limit is imposed by grid spacing, and exhaust velocities below 50 km/s require a heavier propellant, such as cesium or mercury.

A ION THRUSTERS AND POWER PROCESSING

Development of ion thrusters with mercury propellant has been strongly supported by NASA/LeRC for the past 15 years. As a result, these

thrusters are now approaching flight-ready status. The 30-cm (grid diameter) thruster is being readied for primary electric propulsion applications, and smaller devices are expected soon for auxiliary electric propulsion. Figure 1 is a sketch of the 30-cm thruster that has a present mass of 7.3 kg.

The power processing associated with each mercury ion thruster is presently being developed for solar electric propulsion for planetary applications. At a thruster exhaust velocity of 30 km/s, the power processor mass (including structure) is presently 12 kg/kWe. The block diagram for an individual power processor assembly is shown in Fig. 2 (Ref. 4). There are 12 power supplies feeding the thruster in addition to the command, control, switching, and instrumentation functions. Approximately 55% of the mass of this assembly is associated with the accelerator, screen, and discharge supplies that provide 90% of the power to the thruster. The remainder of the supplies (heaters, vaporizers, keepers, and other units) have a mass that tends to be more nearly constant for a given thruster. At very high power levels, these particular power processor components may show a specific mass of less than 1 kg/kWe.

Additional work has been done at LeRC to operate the ion thruster accelerator, screen, and arc discharge directly from solar power inputs. This appears practical for a system that operates at a constant power level, except for a fairly simple control circuitry. However, for stable operation each thruster must be independently coupled to its own power sources.

There has been some disproportionate concern about mercury contamination of the atmosphere with ion thrusters. Actually, more than 90% of the mercury (dependent on utilization efficiency) is expelled by the thruster at Earth escape velocity and will not reenter the biosphere. However, mercury cannot be made available in large annual quantities required for large payload transportation. Argon propellant is available in large quantities and at much lower cost than mercury. Liquid argon can be handled like liquid oxygen as a deep cryogen. Present cost is less than $0.40 per kg, and in large quantity production may be much lower. Of the materials available in larger quantity, argon has the highest atomic mass as well as many other characteristics most desirable for an electric thruster propellant.

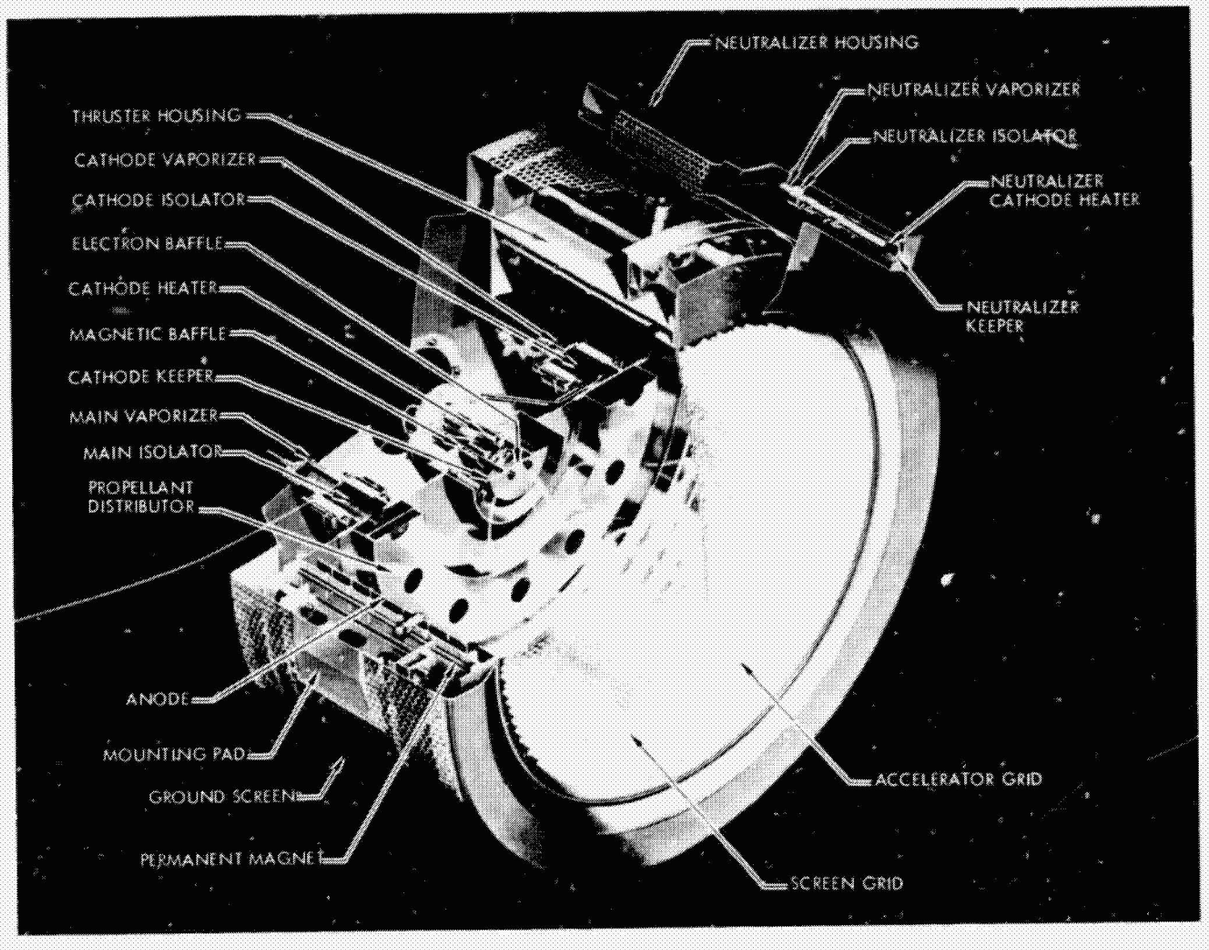

Fig. 1. Electron-bombardment ion thruster

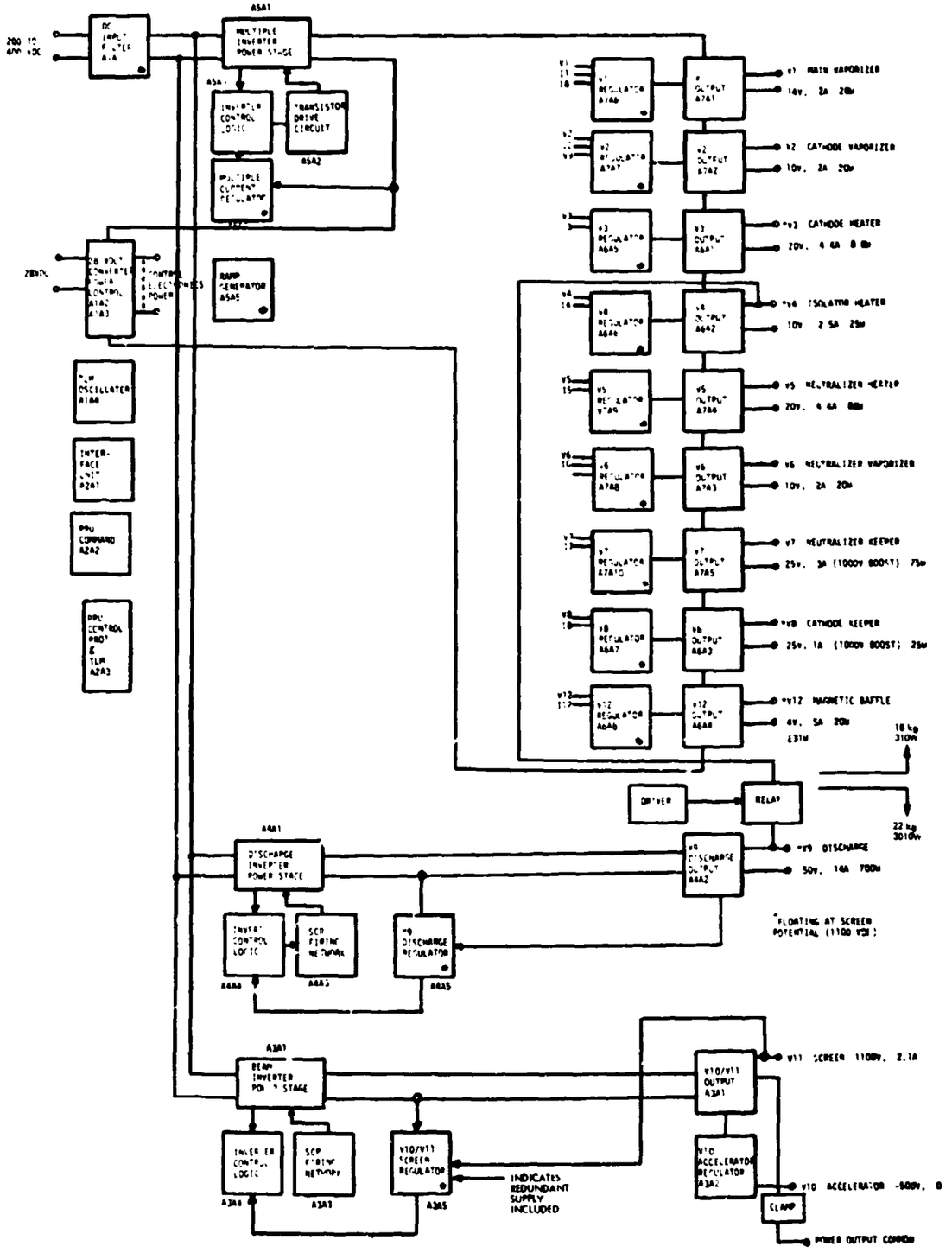

Fig. 2. Ion thruster power processor block diagram

Operation of the ion thruster with argon allows a higher current density than with mercury, but the exhaust velocity (specific impulse) is also higher. At present, maximum propellant utilization is about 0.85, and ionization losses are about 200 eV/ion. This leads to the efficiency curve shown in Fig. 3, compared to the MPD thruster. At an exhaust velocity of 80 km/s, thrust density may be increased to approximately 8 N/m^2, assuming that a thruster operating temperature of 950 K can be achieved.

Figure 4 is a plot of thrust density over a range of exhaust velocities. A major development program will be needed to make flight hardware available, and one of the important considerations in such development is the required heat transfer for high power operation.

Surface emissivity ε of most metals at temperature of 950 K is of the order of 0.5. If the thruster operates at v_e between 60 and 80 km/s, with 0.85 propellant utilization, electrical efficiency is between 0.75 and 0.88. For the thrust levels of Fig. 4, a 50-cm ion thruster would operate at a power level between 45.3 and 83.8 kWe and at a temperature between 900 and 950 K. The area required to dissipate the waste heat (10-11 kWt) is therefore 0.45 - 0.6 m^2. Since the grid area of the ion thruster is approximately 0.2 m^2, additional high-temperature heat rejection area is required.

For the purposes of the study reported here, the 50-cm ion thruster has been selected as the baseline ion thruster. System differences introduced by, say, a 100-cm thruster are negligible. Dished grids with very close spacing have only been developed for the 30-cm thruster. Extrapolation to grid sizes larger than 50-cm diameter is still questionable. Multiple cathodes would also be utilized with the 50-cm thruster.

Operation of the 50-cm thruster with argon rather than mercury is much simpler. Even with the use of multiple cathodes, mass of the 50-cm thruster is now estimated at 6.5 kg. Cost is also reduced by approximately a factor of 3 below the mercury thruster. Although the thruster is very labor-intensive, high production can reduce cost significantly. The final cost of a 50-cm thruster is therefore estimated at $15,000, including cabling and mounting into the thrust subsystem.

Power processors for the ion thruster operating with argon under the above conditions also require new development. For Earth-orbit operation,

the accelerator, screen, and arc discharge operate directly from dc sources (either solar arrays or from transformer/rectifiers). The remainder of the ion thruster requirements will be assumed to be met by processors having a mass of 0.3 - 0.4 kg/kWe, or approximately a factor of 2 better than can be achieved now. In high-quantity mass production, unmanned flight electronics cost could conceivably drop to as low as $800/kg.

B. MPD THRUSTERS AND POWER PROCESSING

An alternative to the ion thruster is the MPD arc thruster, such as shown in Fig. 5. This thruster has a high thrust density (10^5 N/m^2) at an exhaust velocity of 10-50 km/s with argon. Its efficiency, however, is presently estimated at 0.50. Electrical losses are estimated at approximately 5-7% at the cathode and 10% at the anode, and the remainder of the losses are attributed to frozen flow losses. The MPD thruster shown in Fig. 5 operates at a nominal 7.5 MWe, although it may actually be capable of operation up to 10 MWe. There is no experience for thruster operation above 10 MWe, so this is only arbitrarily imposed. Thruster voltage is approximately 200 V, and current is 37,500 to 50,000 A. The tungsten cathode may operate at as high a temperature as 2500-2700 K. The anode and its associated cooling structure is fabricated of molybdenum, operating at a temperature of 1700-1800 K. Several thrusters may apparently be connected in series without control problems, a feature not possible with ion thrusters.

Except for startup and propellant metering, the MPD thrusters need no power processing. Startup requires a low-power, 4000-V pulse to accomplish arc breakdown through the propellant. Stopping may be accomplished by a combination of turning off the propellant feed and switching.

As with the ion thruster, the MPD thruster also requires a large development program before a flight system can be made available. Thermal design for steady-state operation at very high power requires a large effort. A 10-to 20-year lifetime is also needed. The fluid dynamics and the interactions with the magnetic self-field of the arc must be more closely defined for performance optimization. Initial development work might be done with condensable fluids because of the limited gas pumping capacity of existing facilities.

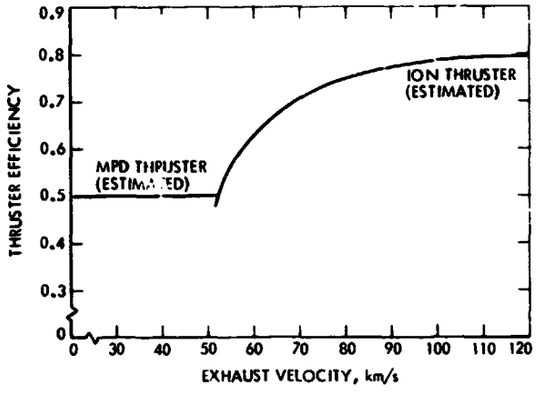

Fig. 3. Electric thruster efficiency with argon propellant

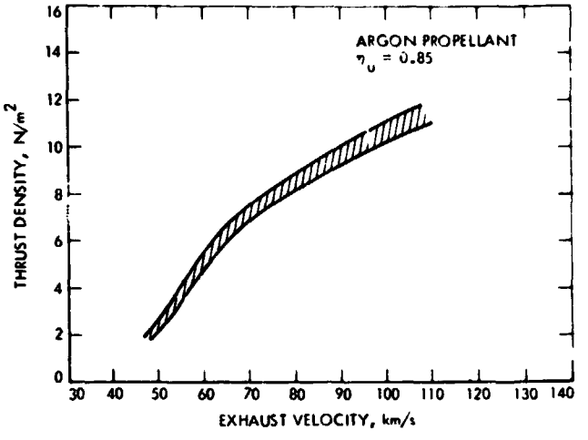

Fig. 4. Advanced ion thruster thrust density

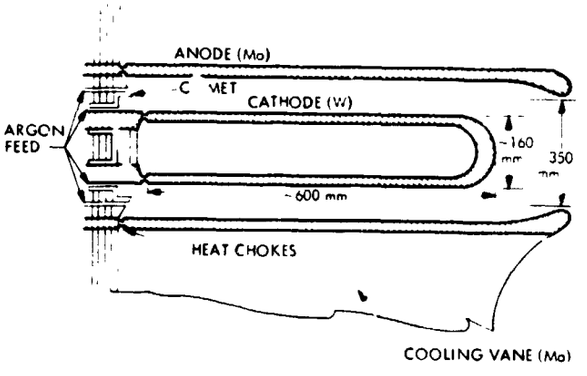

Fig. 5. MPD thruster design concept (7.5 MWe)

The MPD thruster with its cooling fins and associated high-emissivity heat rejection surfaces (3-5 m^2) is expected to have a mass of 350 kg. Because of the unknown problems of high-temperature operation, however, this figure is increased by a factor of 2, to 700 kg. Cost of the thruste. (and its interconnect cabling), also including a safety factor of 2, is approximately $100,000. Power processing, if any, is included, but any transforme. / rectifier requirements for operation from an ac power source are separate.

III. CARGO ORBIT TRANSFER VEHICLE (COTV) MISSION DESIGN

Looking specifically at the mission to place large payloads into GEO, there are two possible approaches. The first is to assemble the payload in LEO and utilize the onboard power for the electric thrusters to raise its orbit to GEO. The second approach is to use a separately powered COTV and assemble the payload in GEO. For the latter, a nuclear electric propulsion (NEP) tug is proposed in this study, although solar arrays capable of operating in the Van Allen belts may also be developed. A further alternative now under study, is to utilize microwave beaming from an orbiting space power platform to the COTV.

A. SELF-POWERED COTV MISSIONS

The lowest-cost OTV mission, NASA studies show (Ref. 5), is obtained by assembling the payload in LEO and utilizing onboard power for propulsion. Low thrust will be necessary because of the lightweight structures. Limitations of thrust acceleration are estimated to lie between 10^{-2} and 10^{-3} m/s^2. Low-thrust spiral trajectories from LEO at 28.5 deg (ETR launch) to GEO have an equivalent Δv of approximately 6200 m/s. An additional 10% is added for gravity-gradient forces and solar pressure, for a total of 6820 m/s.

From an initial 500-km altitude up to 5,100 km, a tangential-thrust spiral is provided at a constant inclination of 28.5 deg. Thereafter, the thrust vector also performs a cross-plane rotation at one revolution per orbit, accomplishing a combined spiral and plane change trajectory. The maneuver is described in detail in Appendix A.

An additional problem of the 28.5 deg initial low-altitude orbit is that a portion of each orbit lies in the Earth's shadow. Studies by the Boeing Aerospace Co. for NASA (Ref. 5) have shown this occultation period is a minimum at solstice (32 min at 500 km altitude, or 34% of orbit). For about the first 25% of the orbit transfer time each spacecraft orbit is partially occulted. During the occultation periods, chemical propulsion must be used, at at least 10% of full thrust, for attitude control. Since chemical propulsion has an order-of-magnitude lower exhaust velocity than the electric thrusters, it is most optimum to minimize the chemical propulsion operation. On the other hand, flight time will be increased by approximately 5% because of the loss of electric power during occultation in low orbit. The value lost because of this longer flight time is yet to be considered. Occultation occurs well into the proton belts, and degradation of the system is increased. Thermal shock and on-off cycling can have significant lifetime implications. However, until further system definition indicates a more desirable optimization a chemical propulsion total Δv contribution of 25 m/s is assumed. The remaining 6795 m/s is provided by the electric propulsion system.

There are several different types of chemical propulsion available, as shown in Table 1. Cost tradeoffs have yet to be made, so any conclusions at this time are definitely premature. However, the higher exhaust velocity of the O_2/H_2 systems (v_e = 4.61 km/s) will probably minimize the launch cost because of less propellant needed in LEO. High-pressure, pump-fed systems are assumed, based on technology being developed by LeRC. Figure 6 is a block diagram of a typical system. Pumps may be powered either by propellant boiloff or by auxiliary electrical battery power. Such systems will have a mass per unit thrust of approximately 250 kg + 0.15 kg/N and will cost approximately $1000 per kg. Chemical propellant mass fraction (m_{pc}/m_0) for a Δv = 25 m/s is 0.0054.

The argon propellant needed for the electric propulsion Δv of 6795 m/s is a function of the exhaust velocity. Mass fraction is shown in Fig. 7. As exhaust velocity increases, propellant mass decreases exponentially. However, mission optimization has additional dimensions. At a fixed power level, flight time increases linearly with exhaust velocity. Power per unit mass may also be varied. These additional dimensions are parameterized in Fig. 8. "Specific power" P_0^* is defined as the power per

unit mass of the initial spacecraft, P/m_0. Since electric thruster efficiency is a variable function of exhaust velocity, jet power P_j ($\eta = 1.0$) is shown here. These curves do not take into account the problem of occultation time delay and assume that the gravity-gradient contribution is a constant 10%. Acceleration levels of 1, 2, 5, and 10×10^{-3} m/s^2 are also plotted on Fig. 8.

System degradation through the proton belts is a first-order mission perturbation. Approximately 70% of the low-thrust transfer time is spent in the proton belts, as may be seen in Fig. 9, up to approximately 15,000 km altitude. Occultation time and gravity gradient variations are not included in the curve. Solar array damage occurs primarily from the fluence of high-energy particles and only secondarily from the total integrated dose. Massive protection would be required to eliminate this damage, even for a flight time of only one day. Since low-thrust trajectories are expected to require at least seven days, the only viable approach is to use radiation-hardened solar arrays.

Standard 12-mil, 10 Ω-cm solar cells will degrade with flight time approximately as shown in Fig. 10. For comparison, a 5-mil "violet" cell is also shown in the figure. The alternative to providing radiation-hardened systems is to take at least a 20-30% power degradation.

B. SEPARATELY POWERED COTV MISSIONS

Assembly in GEO is an alternative mission possibility. Utilization of high thrust, low thrust, or a combination of the two is possible in this case. Multiple round trips are made in order to amortize the cost of the COTV over a much larger payload. For purposes of comparison, a two-stage chemical COTV is first analyzed. Thereafter, we will consider the all-electric and then the combined systems.

1. All-Chemical COTV

The high-thrust Δv required from LEO to GEO is 4300 m/s, or only about 70% of the low-thrust requirement. Optimum staging for two-stage vehicles occurs at approximately equal Δv's, or 2150 m/s per stage. The first-stage system separates and returns to LEO (2150 m/s) for its next

mission load. The second stage provides the remaining Δv (2150 m/s) to place the payload into GEO, and then it also returns to LEO (4300 m/s) for its next mission load. The chemical stages are assumed to use O_2/H_2 propellants at v_e = 4160 m/s and are assumed to have a structural factor λ_s of 0.92. On this basis, the two-stage chemical propulsion mission is summarized in Table 2. The payload fraction of the initial mass in LEO is 0.295. However, 0.055 of the initial mass is in reusable stages, so that, of the remainder, launch vehicle propellant load is 0.688, tankage (at 5% of propellant mass) is 0.034, and payload to LEO is 0.278. Quite probably, a logistics depot in LEO is needed, but is not considered in this analysis.

Cost of actual payload to LEO is $180/kg, based on LLV deliveries at $50/kg Two tug stages are required, and at a service life of 20 round trips cost estimates vary widely among current studies. A median number of $150/kg of GEO payload is assumed here to cover the cost of both tugs, including cost of delivery to LEO. Thus, total transportation cost is estimated at $330/kg for high-thrust chemical propulsion.

No estimate is made of the special manpower and equipment needed for GEO. We assume this to be part of the fabrication and assembly rather than transportation. However, there is undoubtedly a significant additional cost associated with assembly in GEO above that of LEO assembly, and this cost must ultimately be accounted.

2. All-Electric COTV

Low-thrust electric propulsion is the primary competitor to the chemical high-thrust propulsion. Its primary selling point is the higher specific impulse available. However, the spiral trajectory requires 44% higher energy and a much longer flight time. It is because of these drawbacks that many people have taken a careful look at the direct-heating nuclear rocket. But the nuclear rocket also has drawbacks with hydrogen tankage and nuclear safety problems. A two-stage nuclear COTV may also be necessary to compete with the chemical system performance, and the economics of such a system are questionable.

The electric propulsion vehicle is now being conceptually designed for a full-power lifetime of at least 72,000 hours, or 3000 days. Such a system

Table 1. Chemical systems alternatives

Type	Specific impulse
Earth storable	
N_2O_4/N_2H_4	300-315
Pentaborane/N_2H_4	300-400
Space storable	
F_2/N_2H_4	370-390
OF_2/diborane	370-410
Cryogenic	
LO_2/LH_2	425-470

Table 2. Two-stage chemical COTV detail to GEO
(O_2/H_2, one-way Δv = 4300 m/s)

Assumed λ_s	= 0.92
v_e	= 4610 m/s
Staging at Δv	= 2150 m/s
Stage 1	
Propellant mass fraction, m_p/m_0	= 0.40
Inert mass fraction, m_i/m_0	= 0.034
Stage 2	
Propellant mass fraction, m_p/m_0	= 0.25
Inert mass fraction, m_i/m_0	= 0.021
Launch mass fractions	
Payload, 0.278	
Propellant, 0.688	
Tankage, 0.034	
Cost to LEO, $180/kg of payload	

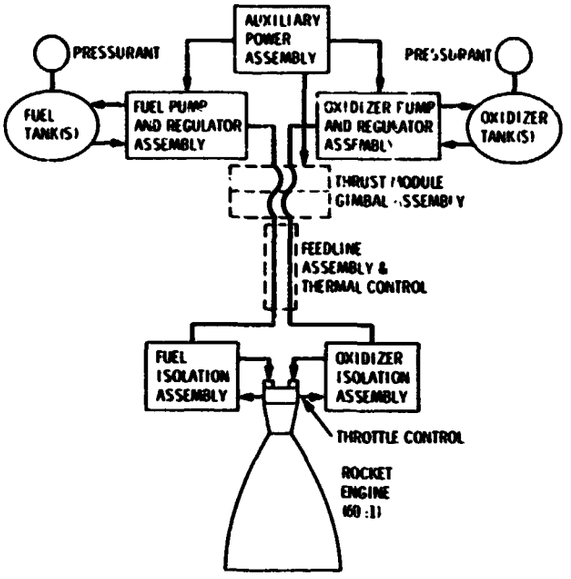

Fig. 6. Block diagram, chemical propulsion subsystem (one of two)

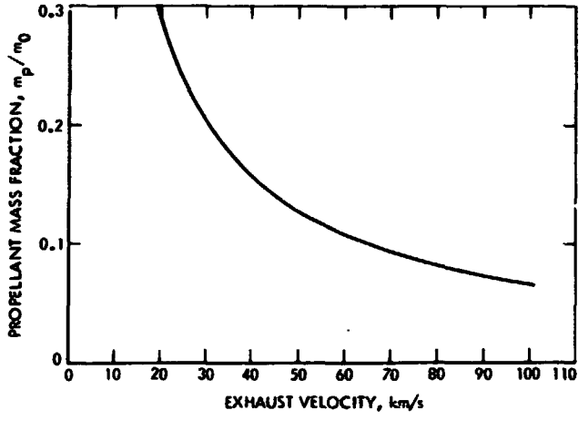

Fig. 7. Low-thrust propellant requirement, one way, LEO to GEO

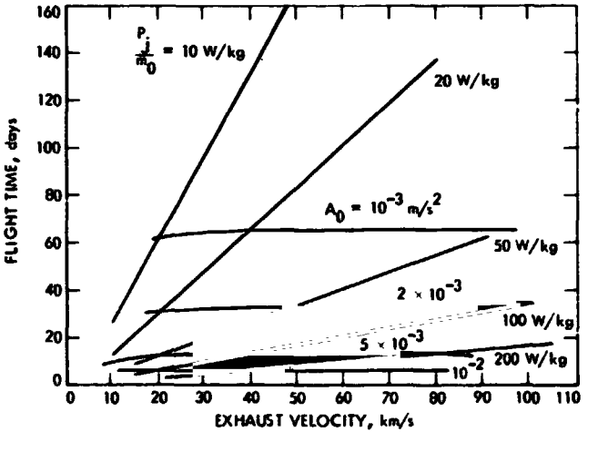

Fig. 8. Orbit transfer time to GEO

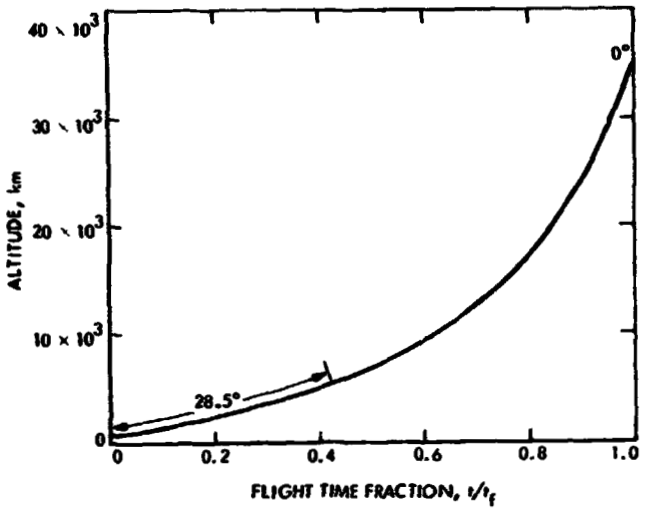

Fig. 9. Spiral trajectory profile to GEO

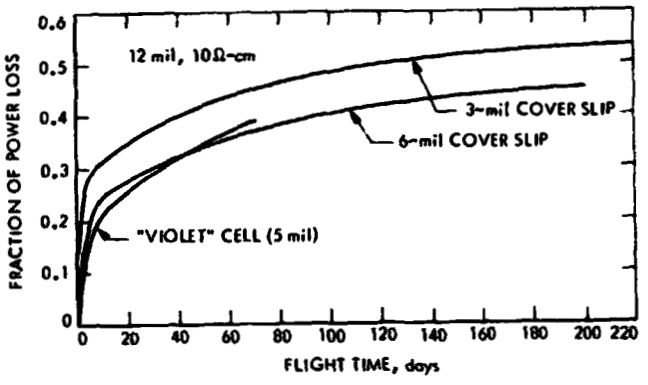

Fig. 10. Silicon solar cell degradation for spiral trajectories to GEO

must be capable of spending relatively long periods within the proton radiation belts. This appears to limit us initially to a nuclear electric system. However, solar power sources may soon evolve for the COTV mission. Since it is still too early for good cost comparisons, we shall consider NEP as our present baseline.

A nuclear power subsystem capable of 1-MWe output is currently being studied for a specific mass estimated at about 18 kg/kWe. Thrust subsystem (exclusive of tankage) and other subsystems for Earth-orbit operation should be no more than $50 million, including a possibly sophisticated teleoperator capability. This vehicle, together with the LLV constitute the transportation system. Performance and cost data are included in Appendix B.

Following the efficiency curves of Fig. 3, cost optimization now appears to be in the exhaust velocity range of 20 to 25 km/s as shown in Fig. 11. This is, however, affected by launch vehicle cost. If the Shuttle were used, at a launch cost of $300-500 per kg, added propellant delivery cost would drive the optimum up to a higher velocity.

For the low-thrust cargo OTV, optimum payload increases (and cost decreases) monotonically with increased flight time. The orbital maneuvering is simple so that navigation is automated and any ground tracking requirements are very slight. The major flight-time limitation will probably be the payload degradation through the Van Allen belts — particularly proton damage. By suitable hardening and packaging techniques, it should be possible to allow flight time of at least a year without serious problems. On this basis, total transportation cost of about $115/kg is achievable with NEP. Payload delivered per trip is 184 metric tons with a 1 MWe tug.

3. Hybrid COTV

The combined high-thrust/low-thrust COTV is a two-stage system that fits, costwise, between the all-chemical and the all-electric systems. The chemical stage delivers payload and propellant to an intermediate orbit, where it is transferred to an electric stage. The electric stage operates between the intermediate orbit and GEO. At the point where chemical Δv exceeds about 3000 m/s, cost of the hybrid COTV becomes larger than the all-chemical system.

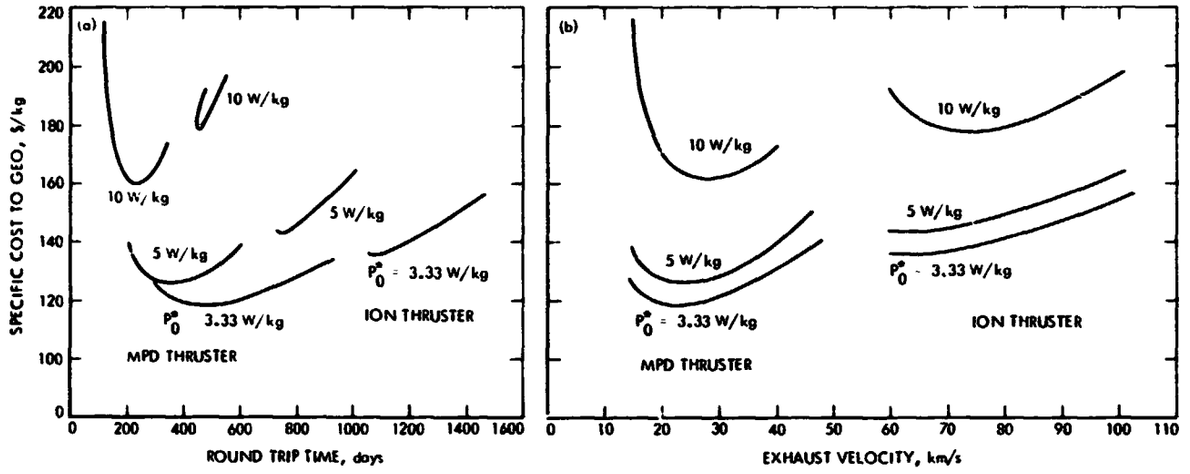

Fig. 11. Transport cost to GEO with reusable NEP Tug and LLV

The hybrid system has very little to recommend it. It is more costly than the all-electric and more complex than either the all-electric or all-chemical.

IV. BASELINE SYSTEM DEFINITION

In the case of large payload assembly in GEO, it is quite evident from the previous section that the all-electric COTV is desired. Cost is lower than chemical COTV by a factor of 3, 40% less than just the launch cost of the all-chemical system. However, its advantage lies in its ability to operate for long periods of time in the proton belts. Optimum exhaust velocity lies in the operating range of the MPD thruster and below the range of the ion thruster. Flight time appears reasonable at an exhaust velocity of 20 km/s (≤1 year).

The main question about assembly in GEO is that of economic tradeoffs with other alternatives. Larger crews and special equipment must be transported in addition to higher transportation costs of payload. Whether this provides adequate incentive for high-cost and high-risk development programs for large payloads must be evaluated on a program-by-program basis.

Cost of space operations is cut approximately in half by assembly in LEO and subsequent low-thrust transport to GEO. Transportation cost may be significantly reduced by using onboard power for propulsion, by eliminating return trips, and by using the thrusters after transport for attitude control and station keeping. In addition, every effort must be made to minimize launch vehicle cost to LEO.

Both the ion thruster and MPD thruster are analyzed in this section of the report. Cost comparisons are made, and recommendations are listed concerning the technology requirements for a viable program. Low cost (including low maintenance) and long lifetime are the drivers.

Both the photovoltaic solar arrays and the solar collector/Brayton systems are potentially available as power sources. A nuclear power system is also being studied, but it suffers from the disadvantage of nuclear fuel processing requirements. The propulsion studies will encompass the constraints of all of these systems and assume that they are all equally

available, with equal performance. For conservatism, a transformer/ rectifier input to the thrust subsystem is assumed at a mass of 7.3/0.04 kg and a cost of $10.7/3.7 per kWe.

A. THRUST SUBSYSTEM ANALYSIS

Thrust subsystems for the self-powered vehicle include electric and chemical propulsion, propellant feed, processing, controls, structure, and heat rejection systems. Several thrust subsystem modules are permanently attached to the spacecraft through two-axis gimbals. Full power is used to propel the system to GEO. Thereafter, low power is used for attitude control and station keeping. Guidance and navigation and other spacecraft functions are associated with the spacecraft.

Materials and structures for large solar arrays in space are not yet developed to the point where proton degradation and array mass and cost can be evaluated. Present technology rollout arrays with 4-mil silicon solar cells (with degradation somewhat lower than that of the 12-mil cells in Fig. 10) have a specific mass of 15 kg/kWe and cost $400/watt. By 1985 it is hoped that spacecraft solar arrays can be developed for 5 kg/kWe and a cost of under $100/W. The A. D. Little concept (Ref. 6) for an array mass under 2 kg/kWe and a cost of $0.30/W requires additional technology breakthrough. Totally new materials for ultra-lightweight, radiation-hardened solar concentrators need to be developed, operating with high-temperature solar cells, probably of the gallium arsenide family. They would see very little degradation in the Van Allen belts. Additional structure, probably of the carbon composite type, would be needed in order to take the thrust loads of the electric propulsion.

For lightweight, low-cost, radiation-hardened arrays, power level would probably want to be a maximum in order to minimize the revenue loss from flight time to GEO. This would, of course, be limited by the structure capability to support the thrust loads, as indicated in Fig. 8.

If the array mass and support structure get heavier, the propulsion exhaust velocity will optimize at a lower level. For thrust-limited structures, power is reduced approximately proportional to the exhaust velocity.

Proton degradation through the Van Allen belts, if silicon cells were necessary, introduces further complications along with mass and cost arguments. Every effort should therefore be made to obtain the lightweight, high-temperature arrays at a very early date. This is a primary factor in reduction of transportation costs.

The ion thrust subsystem module is sketched in Fig. 12. For this configuration we have arbitrarily, for comparison purposes, assumed an electric thrust of 3000 N at an exhaust velocity of 80 km/s. There are 2300 individual ion thrusters (20% redundancy) having the characteristics shown in Table 3. The thrusters, operating at 950 K, are mounted on a 40-meter-diameter structure having a mass of 25,000 kg. Cost of this structure is estimated at $50,000. At the center of this structure are mounted two (redundant) chemical thrusters and appropriate thermal baffles. The structure includes thermal isolation and is cooled at 400 K to allow mounting of power processing equipment on top (the side opposite the thrusters). Power to the thrust module is 160 MWe. Transformer and rectifier assemblies, operating at respective efficiencies of 0.99 and 0.995, have respective masses of 120,000 and 6500 kg. Additional power processing is approximately 49,000 kg. Cruciform heat-rejection heat pipe radiators operate at 400 K for rectifier and power processor cooling and at 600 K for transformer cooling. Total radiating surface area of 2130 m^2 is needed. Cost is estimated at $1950/$m^2$, or $4.16 million. The majority of the central structure of the module is provided by the transformer, approximately 6 m high by 2 m diameter. The end-to-end radiator wingspan is 90 m. Heat rejection assemblies have a total mass of 33,000 kg.

The thrust modules are attached to the spacecraft through gimbals in order to provide attitude control. Large masses are involved, but thrust levels are relatively small and angle changes are relatively slow. Torque demands, therefore, are only of the order of 300 N-m maximum. This is, however, superimposed on a thrust level of 3000 N. Thus it is necessary to operate the thrusters such that they produce no average moment about the gimbals. Vernier gimballing of thrusters, variable thrust control, and/or preset alignment and switching of thrusters are alternate methods of aiding in the process of net torque elimination.

Each thrust subsystem module is expected to require two axes of controlled gimbal motion through respective angles of $\pm\pi/2$ and $\pm\pi/4$ radians. Redundant pairs of digitally operated stepper motors are mounted through a gear train on each gimbal axis (Ref. 7). Appropriate mechanical disconnect is needed in case of component failure. Direction of motion and torquing directions with respect to gravity gradient torques, orbit inclination and solar alignment must all be studied in detail in future studies. Until detailed dynamic analyses can be completed, maximum versatility is to be maintained in the thrust subsystem module design.

Propellant tankage is mounted on the main spacecraft rather than on the module. Propellants are carried past the thrust subsystem gimbals through multiple pressurized flex lines. Flexible (copper) cabling is similarly provided for multiple electric power lines at 200-500 kV. Instrumentation and control circuitry is also provided. Minimum cost switching and logic is mounted on the thrust subsystem module as well as simple onboard engineering data handling. Emphasis should be to reduce complexity across the gimbal.

There are 25 thrust subsystem modules mounted at various positions about the 4000-MWe self-powered spacecraft. Mission performance and cost are summarized later.

As an alternative, the MPD thrust subsystem module is sketched in Fig. 13. Again, an electric thrust of 3000 N is arbitrarily assumed, but at an exhaust velocity of 25 km/s. Ten individual MPD thrusters operate with the characteristics of Table 3. The thrusters, operating at 1700 K, are mounted on a 6-meter-diameter structure having a mass of 5000 kg, including thermal control, and a cost of \$10,000. Two chemical thrusters are mounted in the center, as in the ion thruster concept above. Power to the electric thrusters is 75 MWe. Transformers and rectifiers (including control circuitry) are provided as before, with masses of 55,000 and 3000 kg, respectively, and cost of \$800,000 and \$280,000, respectively. Heat rejection surface area is 512 m^2. For a 6-m height, this requires a radiator wingspan of 22 m (including the 1-m-diameter transformer at the center). Mass of the heat rejection system is 8000 kg at a cost of \$1 million. A total of 53 of the MPD thrust subsystem modules is attached to the 4000-MWe spacecraft.

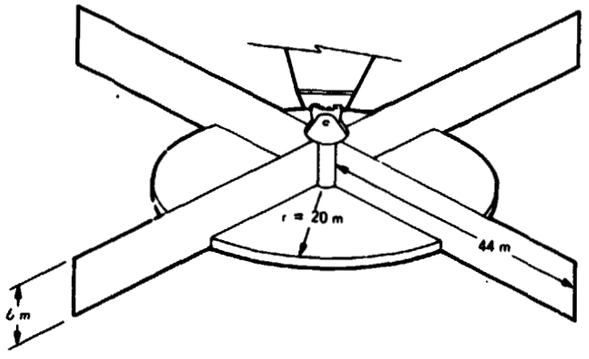

Fig. 12. Ion thrust subsystem (module) configuration

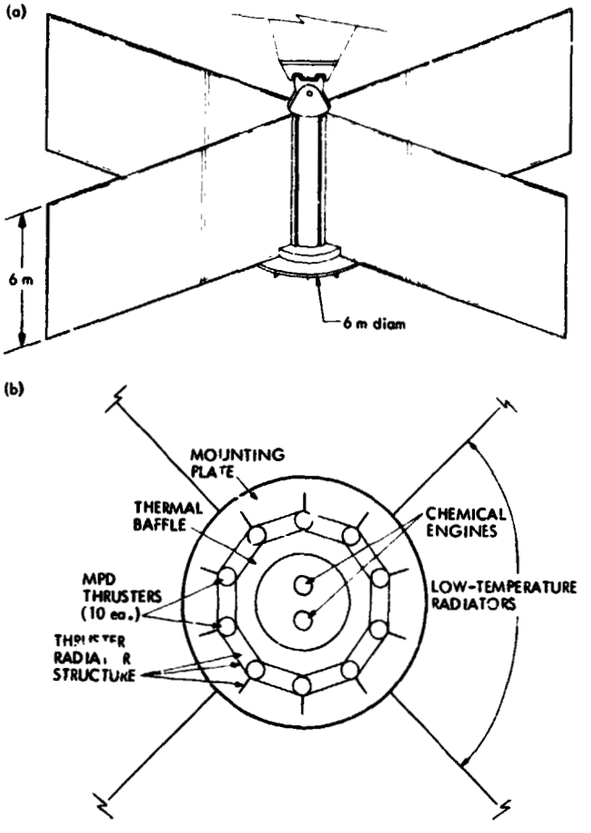

Fig. 13. MPD thrust subsystem (module) configuration

Table 3. Electric thruster characteristics

A. 50-cm ion thrusters			
Exhaust velocity, km/s	60	80	100
Efficiency	0.63	0.75	0.785
Power input, kWe	40.5	83	146.5
Thrust, N	0.85	1.55	2.3
Mass, kg	6.5	6.5	6.5
Temperature, K	900	950	950
Cost, $k	15	15	15
B. 7.5-MWe MPD thruster			
Exhaust velocity, kw/s	10	25	50
Efficiency	0.5	0.5	0.5
Power input, kWe	7500	7500	7500
Thrust, N	750	300	150
Mass, kg	700	700	700
Temperature, K	1700	1700	1700
Cost, $k	100	100	100

Performance comparisons between the ion thruster and MPD thruster subsystems can be seen in Fig. 14. Since the specific mass of the spacecraft is not yet defined, it is shown parametrically. We have assumed that all spacecraft power generated is used for propulsion during orbit transfer. The parameter of specific mass in Fig. 14 is for the spacecraft only in LEO. It is exclusive of thrust subsystem mass, tankage, and propellants. This allows direct performance comparison between the ion and MPD thrust subsystems.

It should be noted in the performance comparisons that the two types of electric thrusters complement each other very well over the wide range of specific impulse covered. The MPD thruster will operate well between 10 and 50 km/s, but has not been proven at higher exhaust velocity. The ion thruster with argon propellant does not operate well below 50 km/s.

B. TRANSPORTATION COST ANALYSIS

Baseline system selection between the ion and MPD thruster is to be made on the basis of cost. The main spacecraft and the chemical propulsion are assumed the same for both electric systems.

The cost of degradation through the Van Allen belts reflects into a requirement for a larger array, and thus a heavier array than would otherwise be built. It is therefore important to eliminate this degradation if at all possible. Another cost to be reckoned is that of loss of revenue as a function of flight time. Rate to be charged is controversial, but it should at least include the return of invested cost. On the low side, \$0.020/kW-h is assumed. Thus, the 4-GWe spacecraft module delivers 2.5×10^6 kW through a microwave link at a cost of \$1.2 million per day. For a spacecraft module mass of $40\text{-}60 \times 10^6$ kg, this is not a major cost item unless flight time becomes very large.

The 4-GWe spacecraft is assumed to have a specific mass of 5, 10, and 15 kg/kWe. Costs are applied and results tabulated in Appendix C. Cost summary is plotted in Figs. 15 and 16. Cost of argon was assumed at \$0.40/kg, and argon tankage at \$200/kg.

There is a clear advantage for the MPD thruster shown in this analysis. This advantage becomes more distinct as solar power degradation increases.

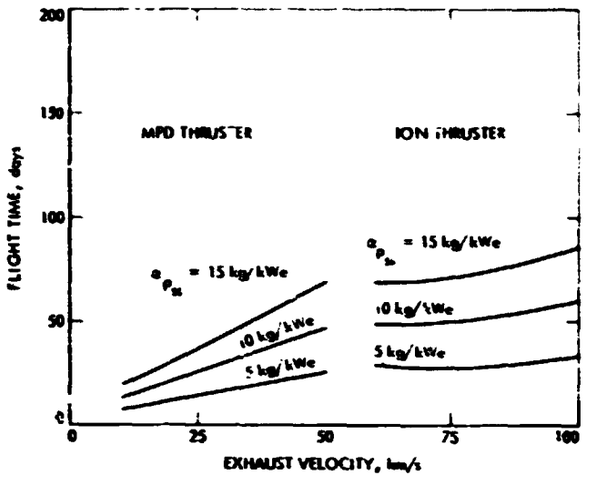

Fig. 14. Electric thrust flight time performance (one way self-powered missions to GEO)

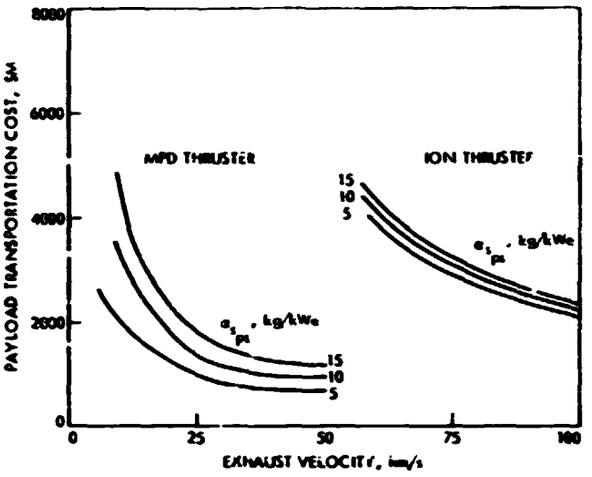

Fig. 15. Transport cost, LEO to GEO, with self-powered SEP

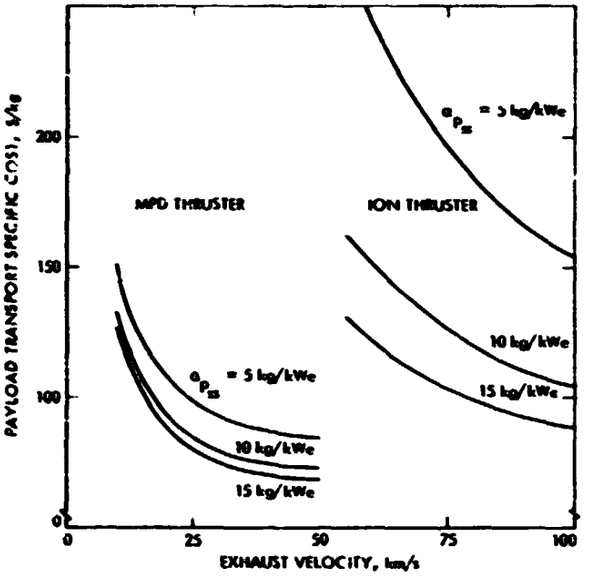

Fig. 16. Transport specific cost to GEO with self-powered SEP

These conclusions are substantiated by recent progress reports in the contracted studies by the Boeing Aerospace Co. previously referenced. Compared to costs shown in Fig. 11, the cost of this method of transportation is nearly half the cost of that for assembly in GEO, and flight time is very much shortened.

V. CONCLUSIONS AND RECOMMENDATIONS

1. A Large Lift Vehicle (LLV), capable of delivering mass to LEO at a cost of less than $50 per kg is essential for large, low-cost payloads in Earth orbit. The cost of delivery to LEO is the primary cost of space transportation.

2. Assembly of large payloads in LEO and use of onboard power for subsequent delivery to GEO can reduce cost by a factor of 3 compared to assembly in GEO. This requires large, lightweight structure capable of thrust loads of 10^{-3} to 10^{-2} m/s while maintaining solar orientation.

3. Radiation-hardened solar arrays are vital for achieving a 20- to 30-year lifetime in the space environment and for low-thrust transfer through the Van Allen belts. Presently available technology, even the thin silicon cell, appears inadequate. Advanced concepts including special dopants, surface treatment, new materials (GaAs), and concentrators need development. Low cost, high production capability is a major driver.

4. MPD thrust subsystem technology is needed by approximately 1983-1985, when major programs are expected to start. Short flight time, low cost, and system simplicity compared to other alternatives are major contributions of these thrusters to economical Earth-orbit transportation.

5. Argon propellant production capability is required near the LLV launch site. Production capacity should be approximately 10^6 kg/year by 1985, increasing to 10^8 kg/year by 1990.

APPENDIX A

LOW-THRUST EARTH-ORBIT SPIRAL TRAJECTORIES

I. EQUATIONS OF MOTION

Based on Ref. 8, a set of equations have been developed to define low-thrust operation in geocentric space. This definition involves spiral trajectories between an initial orbit r_0 and a final orbit r. Plane changes ϕ, in radians, may also be accomplished, either separately or in combination with orbit raising.

The low-thrust spiral trajectories can be expressed by

$$\frac{r}{r_0} = \frac{1}{\left[1 + \frac{1}{\nu} \ln\left(1 - \frac{a_0 t}{v_e}\right)\right]^2} \qquad \text{(A-1)}$$

where

$$\nu = \frac{\sqrt{\mu / r_0}}{v_e}$$

$$a_0 = \frac{2\eta P}{m_0 v_e}$$

r = final radius

r_0 = initial radius

v_e = thruster exhaust velocity

μ = earth gravitational constant

t = thrust time

a_0 = initial thrust acceleration

m_0 = initial mass

η = propulsion efficiency

P = propulsion power

It is also possible to express plane changes by

$$\phi = \frac{2v_e}{\pi\sqrt{\mu/r}} \frac{1}{\ln\left(1 - \frac{a_0}{v_e} t\right)} \tag{A-2}$$

If each of the functions is performed separately, the time for given orbit raising and angle change would be

$$t_r = \frac{\left[1 - e^{-\nu(1 - \sqrt{r_0/r})}\right] v_e}{a_0} \tag{A-3}$$

and

$$t_\phi = \frac{\left[1 - e^{-\nu\pi\phi/2}\right] v_e}{a_0} \tag{A-4}$$

But it is also possible, through a very simple programmed rotation of the spacecraft, to rotate the thrust vector at one revolution per orbit and thereby perform a simultaneous orbit raising and plane change maneuver. This combined maneuver will take less time than performing each maneuver separately. The angular change bears a fixed relationship to the radius change:

$$\phi(r) = \frac{\pi}{8} \ln\left(\frac{r}{r_0}\right) \tag{A-5}$$

and the time required to perform this combined maneuver is given by

$$t_c = \frac{\left[1 - e^{-\nu(1 - \sqrt{r_0/r})}\right] \pi v_e}{2\, a_0} \tag{A-6}$$

It is desirable to make orbit plane changes at maximum radius, since angular rate is proportional to $\sqrt{r}$. If required plane change is less than that of Eq. (A-5), a direct spiral via Eq. (A-3) should be utilized to raise r_0' to the proper value, and therefore utilize the combined maneuver via Eq. (A-6). For a larger plane change than Eq. (A-5), utilize the combined maneuver, Eq. (A-6), up to maximum r, and then utilize Eq. (A-4) for the remainder of the plane change.

II. GEOSYNCHRONOUS EQUATORIAL ORBIT ANALYSIS (GEO)

Shuttle has been previously designed for maximum low earth orbit (LEO) altitude of 500 km (270 nm) or an orbital radius of 6880 km. We shall also assume the initial orbit of the launch vehicle to be inclined 28.5° from the equator (i.e., a due east launch from ETR). From Eq. (A-5), therefore, we find that the lower radius for the combined maneuver, r_0', is 11,886 km. Equation (A-3) is thus utilized up to this radius and Eq. (A-6) is utilized thereafter.

It is further possible to normalize the equations with respect to power level and initial mass, since both of these are included only in a_0. Thus, the results may be expressed in power time per unit mass, MWe-s-kg^{-1}. For any given propellant exhaust velocity, propellant expenditure is independent of power level and directly proportional to the initial mass. The propellant mass flow rate is

$$\dot{m} = \frac{2\eta P}{v_e^2} \tag{A-7}$$

The final equations for geosynchronous equatorial orbit ($r = 42,184$ km) are therefore

$$\frac{P}{m_0} t_r = \frac{v_e^2}{2\eta} \left[1 - e^{-v_0 \left(1 - \sqrt{r_0/r_0'}\right)}\right] \tag{A-8}$$

and

$$\frac{P}{m_0} t_c = \frac{\pi v_e^2}{4\eta} e^{-\nu_0 \left(1 - \sqrt{r_0/r_0'}\right)} \left[1 - e^{-\nu_0 \sqrt{r_0/r_0'} \left(1 - \sqrt{r_0'/r}\right)}\right] \quad \text{(A-9)}$$

If v_e is expressed in km/s, and P is in MWe, Eqs. (A-8) and (A-9) evaluate to:

$$\frac{P}{m_0} t_r = \frac{v_e^2}{2\eta} (1 - e^{-x}) \quad \text{(A-8a)}$$

and

$$\frac{P}{m_0} t_c = \frac{\pi v_e^2}{4\eta} e^{-x} (1 - e^{-y}) \quad \text{(A-9a)}$$

where

$$x = \frac{1.8206}{v_e}, \quad y = \frac{2.717}{v_e}$$

Time to synchronous orbit, normalized for power and mass, is thus

$$\frac{P}{m_0} t_s = \frac{v_e^2}{2\eta} \left[1 - e^{-x} \left(1 - \frac{\pi}{2} + \frac{\pi}{2} e^{-y}\right)\right] \quad \text{(A-10)}$$

For values of $y << 1$,

$$\left(1 - \frac{\pi}{2} + \frac{\pi}{2} e^{-y}\right) \cong e^{-\frac{\pi}{2} y} \quad \text{(A-11)}$$

The propellant expended to GEO is then

$$\frac{m_{ps}}{m_0} \cong 1 - e^{-x}\, e^{-\frac{\pi}{2} y} \tag{A-12}$$

and the payload delivered to GEO is

$$\frac{m_L}{m_0} \cong e^{-x}\, e^{-\frac{\pi}{2} y} - \frac{m_w}{m_0} \tag{A-13}$$

where

m_L = payload mass to GEO

m_0 = initial mass in LEO

m_w = propulsion inert mass

Furthermore, by combining Eqs. (A-10) and (A-12), it is possible to express payload as a function of time:

$$\frac{m_L}{t_s} \cong \frac{2\eta P}{v_e^2}\left[\frac{e^{-x}\, e^{-\frac{\pi}{2} y} - \frac{\alpha P}{m_0}}{1 - e^{-x}\, e^{-\frac{\pi}{2} y}}\right] \tag{A-14}$$

where

$$\alpha = \frac{m_w}{P} = \text{specific mass of the propulsion system}$$

For this mission the equivalent velocity increment can now be calculated:

$$\Delta v_{equiv.} \cong -v_e \ln\left[e^{-x}\left(1 - \frac{\pi}{2} + \frac{\pi}{2} e^{-y}\right)\right] \tag{A-15}$$

or, for $y << 1$,

$$\Delta v_{equiv.} \cong v_e \left(x + \frac{\pi}{2} y\right) \cong 6.1 \text{ km/s} \qquad \text{(A-15a)}$$

APPENDIX B

NUCLEAR ELECTRIC TUG PERFORMANCE AND TRANSPORTATION COST ANALYSIS

One alternative COTV concept for assembly of large systems in GEO is to utilize a NEP Tug. Either ion thrusters or the MPD thrusters may be used. The NEP will pick up payload and propellant in LEO, carry the payload up to GEO, and then return empty to LEO for another load. The propellant tankage is assumed to be approximately 5% of the propellant mass. Transport time is dependent on the exhaust velocity v_e and the power-to-initial mass ratio $P/m_0 = P^*$, and is given by the expression:

$$t = \frac{m_p}{\dot{m}_0} = \frac{m_p/m_0}{2\eta P^*/v_e^2}, \qquad \text{(B-1)}$$

where

m_p/m_0 = propellant mass fraction (round trip)

η = propulsion efficiency

P^* = specific power, W/kg

v_e = propellant exhaust velocity

Total lifetime of the NEP Tug is assumed to be 70,000 full power hours, or 2916.67 days.

Transport cost includes cost of Tug and launch cost of payload, propellant, and Tug to LEO. Costs are amortized over the payload delivered to GEO for the entire life of the Tug.

Table B-1 covers the MPD thruster for exhaust velocities between 10 and 50 km/s. Table B-2 covers the ion thruster at exhaust velocities between 60 and 100 km/s. Specific power levels of 3.33, 5, and 10 are assumed. Both the LLV launch cost of \$50/kg and the Shuttle launch cost of \$300-500/gk are shown.

Tug cost is assumed to be \$50 × 10^6/MWe, or \$50/We. This cost is amortized over the entire payload delivered or

$$\text{Tug cost, \$/kg} = \frac{50P^*}{\Sigma m_L/m_0} \tag{B-2}$$

where

m_L/m_0 = payload mass fraction

Cost per unit mass of payload to LEO is the cost of transport of payload and propellant, at \$50/kg, divided by the mass of payload. NEP Tug mass is subtracted and considered separately in the following:

$$\text{Payload cost to LEO, \$/kg} = 50\left(1 - \frac{\alpha' P^*}{m_L/m_0}\right) \tag{B-3}$$

$$\text{Tug cost to LEO, \$/kg} = \frac{50}{\text{No. of R.T.}}\left(\frac{1}{m_L/m_0} - 1\right) \tag{B-4}$$

where

α' = specific mass of NEP Tug, kg/We

Table B-1. MPD thruster performance and cost

P*, W/kg	v_e, km/s	m_L/m_0	Days R.T.	No. of R.T.	$\sum \frac{m_{PL}}{m_0}$	Tug, $/kg	LEO, $/kg	Tug to LEO	Total, $/kg
				LLV at $50/kg					
3.33	15	0.516	303	9.62	4.97	33.55	87.48	4.88	125.91
	20	0.608	417	7.0	4.25	39.19	74.62	4.60	118.41
	25	0.667	531	5.47	3.64	45.75	68.30	4.56	118.61
	30	0.706	646	4.52	3.19	52.26	64.60	4.61	121.47
	40	0.758	877	3.33	2.52	66.11	60.38	4.79	131.28
5.0	15	0.457	212	13.76	6.28	39.78	94.55	4.32	138.65
	20	0.555	291	10.02	5.56	44.94	78.22	4.00	127.16
	25	0.617	370	7.88	4.86	51.45	70.68	3.94	126.07
	30	0.664	449	6.50	4.31	57.97	65.86	3.89	127.72
	40	0.713	609	4.79	3.41	73.25	61.50	4.20	138.95
10.0	15	0.277	122	23.91	6.62	75.53	134.64	5.46	215.63
	20	0.396	165	17.66	6.98	71.60	94.98	4.32	170.90
	25	0.467	211	13.82	6.45	77.48	80.82	4.13	162.43
	30	0.516	255	11.46	5.91	84.64	73.45	4.09	162.18
	40	0.577	343	8.52	4.92	101.69	65.88	4.30	171.87
				Shuttle at $300/kg					
3.33	15					33.55	524.88	29.28	587.71
	20					39.19	447.72	27.60	514.51
	25					45.75	409.80	27.36	482.91
	30					52.26	387.60	27.66	467.52
	40					66.11	362.28	28.74	457.13

Table B-1 (contd)

P*, W/kg	v_e, km/s	m_L/m_0	Days R.T.	No. of R.T.	$\sum \frac{m_{PL}}{m_0}$	Tug, $/kg	LEO, $/kg	Tug to LEO	Total, $/kg
				Shuttle at $300/kg (contd)					
5.0	15					39.78	567.30	25.92	633.00
	20					44.94	469.32	24.00	538.26
	25					51.45	424.08	23.64	499.17
	30					57.97	395.16	23.34	476.47
	40					73.25	369.00	25.20	467.45
10.0	15					75.53	807.84	32.76	916.13
	20					71.60	569.88	25.92	667.40
	25					77.48	484.92	24.78	587.18
	30					84.64	440.70	24.54	549.88
	40					101.69	395.28	25.80	522.77
				Shuttle at $500/kg					
3.33	15					33.55	874.80	48.80	957.15
	20					39.19	746.20	46.00	831.39
	25					45.75	683.00	45.60	774.35
	30					52.26	646.00	46.10	744.36
	40					66.11	603.80	47.90	717.81

Table B-1 (contd)

P*, W/kg	v_e, km/s	m_L/m_0	Days R.T.	No. of R.T.	$\sum \frac{m_{PL}}{m_0}$	Tug, $/kg	LEO, $/kg	Tug to LEO	Total, $/kg
					Shuttle at $500/kg				
5.0	15					39.78	945.50	43.20	1028.48
	20					44.94	782.20	40.00	867.14
	25					51.45	706.80	39.40	797.65
	30					57.97	658.60	38.90	755.47
	40					73.25	615.00	42.00	730.25
10.0	15					75.53	1346.40	54.60	1476.53
	20					71.60	948.80	43.20	1064.60
	25					77.48	808.20	41.30	926.98
	30					84.64	734.50	40.90	860.04
	40					101.69	658.80	43.00	803.49

Table B-2. Ion thruster performance and cost

P*, W/kg	v_e, km/s	m_L/m_0	Days R.T.	No. of R.T.	$\sum \frac{m_{PL}}{m_0}$	Tug, $/kg	LEO, $/kg	Tug to LEO	Total, R/kg
				LLV at $50/kg					
3.33	60	0.811	1063	2.75	2.23	74.88	56.59	4.25	135.72
	80	0.838	1201	2.43	2.04	81.88	54.82	3.98	140.68
	100	0.858	1443	2.02	1.73	96.43	53.59	4.08	154.10
5.0	60	0.768	737	3.96	3.04	82.27	57.52	3.82	143.61
	80	0.797	831	3.51	2.79	89.46	55.27	3.64	148.37
	100	0.814	998	2.92	2.38	105.11	54.15	3.91	163.17
10.0	60	0.640	478	6.10	3.90	128.05	59.66	4.61	192.32
	80	0.672	462	6.32	4.24	117.79	56.94	3.87	178.60
	100	0.691	553	5.27	3.64	137.25	56.42	4.24	196.91
				Shuttle at $300/kg					
3.33	60					74.88	339.54	25.50	439.92
	80					81.88	328.92	23.88	434.68
	100					96.43	321.54	24.48	442.45
5.0	60					82.46	345.12	22.92	450.50
	80					89.46	331.62	21.84	442.92
	100					105.11	324.90	23.46	453.47
10.0	60					128.05	357.96	27.66	513.67
	80					117.79	341.64	23.22	482.65
	100					137.25	332.52	25.44	495.21

Table B-2 (contd)

P_{in}, W/kg	v_e, km/s	m_L/m_0	Days R.T.	No. of R.T.	$\sum \frac{m_{PL}}{m_0}$	Tug, $/kg	LEO, $/kg	Tug to LEO	Total, R/kg
				Shuttle at $500/ig					
3.33	60					74.88	565.90	42.50	683.28
	80					81.88	548.20	39.80	673.28
	100					96.43	535.90	40.80	673.13
5.0	60					82.46	575.20	38.20	695.86
	80					89.46	552.70	36.40	678.56
	100					105.11	541.50	39.10	685.71
10.0	60					128.05	596.60	46.10	770.75
	80					117.79	569.40	38.70	725.89
	100					137.25	554.20	42.40	733.35

APPENDIX C

SELF-POWERED SPACECRAFT ORBIT TRANSFER COST ANALYSIS

Based upon a 4-GWe spacecraft power subsystem, having a specific mass of 5, 10, and 15 kg/kWe, transportation costs are modeled for a one-way trip to GEO. Both the MPD thrust subsystem and the ion thrust subsystem are analyzed. Cost includes cost of hardware and propellants and also the launch cost to LEO (at $50/kg).

Taken from the main part of this report, hardware cost and mass per MWe are listed in Tables C-1. Total subsystem costs and masses are then shown in Tables C-2 and C-3. Flight times are listed in Table C-4, based on a total mission Δv of 6795 m/s:

$$t_f \geq \frac{v_e^2}{2\eta P^*} \left(1 - e^{-\Delta v / v_e}\right) \qquad \text{(C-1)}$$

where

v_e = propellant exhaust velocity

$P^* = P/m_0$ = specific power (per unit initial mass) to the propulsion subsystem

η = propulsion efficiency

Finally, Table C-5 is a tabulation of transportation cost as a function of exhaust velocity/flight time for each value of power subsystem specific mass.

Table C-1. Electric thrust subsystem costs

Item	Cost per MWe, $k			Mass per MWe, kg		
MPD thrust subsystems (constant efficiency)						
Thrusters and cabling	13.3			93.33		
Mounting structure	0.13			66.33		
Transformer assemblies	10.7			733.33		
Argon feed systems	0.67			2.75		
Heat rejection systems	13.3			106.33		
Power processing	3.7			40.0		
Ion thrust subsystems						
v_e =	60	80	100	60	80	100
Thrusters and cabling	444	216	125	192	93.75	54.5
Mounting structure	0.6	0.3	0.2	322	156	85.3
Transformer assemblies	10.7	10.7	10.7	733	733	733
Argon feed systems	0.7	0.5	0.4	1.5	1.0	0.75
Heat rejection systems	13.3	13.3	13.3	206	206	206
Power processing	311	282	241	390	352	302

Table C-2. MPD thruster subsystem cost and mass parameters (4000 MWe)

Electric assemblies	v_e = 10 km/s			v_e = 25 km/s			v_e = 50 km/s		
	Cost, $M		Mass,	Cost, $M		Mass,	Cost, $M		Mass,
	Hardware	To LEO	kg × 10^6	Hardware	LEO	kg × 10^6	Hardware	LEO	kg × 10^6
Thrusters and cabling	53.3		0.373	53.3		0.373	53.3		0.373
Mounting structure	0.5		0.267	0.5		0.267	0.5		0.267
Transformer assemblies	42.7		2.933	42.7		2.933	42.7		2.933
Argon feed systems	2.7		0.011	2.7		0.011	2.7		0.011
Heat rejection systems	53.3		0.427	53.3		0.427	53.3		0.427
Power processing	14.9		0.160	14.9		0.160	14.9		0.160
	167.4	208.5	4.171	167.4	208.5	4.171	167.4	208.5	4.171
Chemical assemblies	15.7		0.0157	15.7		0.0157	15.7		0.0157
Auxiliary assemblies	64		0.021	64		0.021	64		0.021
	79.7	1.8	0.0367	79.7	1.8	0.0367	79.7	1.8	0.0367
	247.1	210.3	4.2077	247.1	210.3	4.2077	247.1	210.3	4.2077
Propellants									
Argon at 5 kg/kWe	1.0	1239.2	24.78	0.3	384.5	7.69	0.1	177.7	3.55
10 kg/kWe	1.8	2261.8	45.24	0.6	701.7	14.03	0.3	324.3	6.49
15 kg/kWe	2.6	3284.4	65.69	0.8	1019.0	20.38	0.4	470.9	9.42
O_2/H_2 at 5 kg/kWe	0.2	6.9	0.138	0.2	6.6	0.133	0.2	6.6	0.132
10 kg/kWe	0.3	12.6	0.251	0.3	12.2	0.243	0.3	12.0	0.241
15 kg/kWe	0.5	18.3	0.365	0.5	17.6	0.353	0.5	17.5	0.350
Tankage (0.05 Mp)									
Argon at 5	247.8	62.0	1.24	76.9	19.2	0.385	35.5	8.9	0.178
10	452.4	113.1	2.26	140.3	35.1	0.702	64.9	16.2	0.325
15	656.9	164.2	3.28	203.8	51.0	1.019	94.2	23.6	0.471
O_2/H_2 at 5	1.4	0.3	0.007	1.3	0.3	0.007	1.3	0.3	0.007
10	2.5	0.6	0.013	2.4	0.6	0.012	2.4	0.6	0.012
15	3.7	0.9	0.018	3.5	0.9	0.018	3.5	0.9	0.018

Table C-3. Ion thruster subsystem cost and mass parameters (4000 MWe)

Electric Assemblies		v_e = 60 km/s			v_e = 80 km/s			v_e = 100 km/s		
		Cost $M		Mass,	Cost, $M		Mass,	Cost, $M		Mass,
		Hardware	To LEO	kg x 10^6	Hardware	LEO	kg x 10^6	Hardware	LEO	kg x 10^6
Thrusters and cabling		1775		0.769	862.5		0.375	502.6		0.218
Mounting structures		2.6		1.287	1.3		0.625	0.7		0.341
Transformer assemblies		42.7		3.000	42.7		3.000	42.7		3.000
Argon feed systems		2.7		0.006	2.0		0.004	1.6		0.003
Heat rejection systems		53.3		0.825	53.3		0.825	53.3		0.825
Power processing		1245		1.558	1128		1.410	965		1.206
		3122.3	372.3	7.445	2089.8	312.0	6.239	1565.9	279.7	5.593
Chemical assemblies		15.7		0.0157	15.7		0.0157	15.7		0.0157
Auxiliary assemblies		64		0.021	64		0.021	64		0.021
		79.7	1.8	0.0367	79.7	1.8	0.0367	79.7	1.8	0.0367
		3202.0	374.1	7.482	2169.5	313.8	6.276	1645.6	281.5	5.630
Propellants										
Argon	5	0.16	201.5	4.03	0.09	116.9	2.34	0.07	90.4	1.81
	10	0.28	348.1	6.96	0.16	206.0	4.12	0.13	160.9	3.22
	15	0.40	494.8	9.90	0.24	295.0	5.90	0.19	231.5	4.63
Chemical	5	0.20	7.5	0.150	0.19	7.1	0.143	0.18	7.0	0.139
	10	0.34	12.9	0.259	0.33	12.6	0.251	0.33	12.4	0.248
	15	0.48	18.4	0.368	0.47	18.0	0.360	0.47	17.8	0.356
Tankage (at 0.05 Mp)										
Argon	5	40.3	10.1	0.202	23.4	5.9	0.117	18.1	4.5	0.091
	10	69.6	17.4	0.348	41.2	10.3	0.206	32.2	8.1	0.161
	15	99.0	24.8	0.495	59.0	14.8	0.295	46.3	11.6	0.232
Chemical	5	1.5	0.4	0.008	1.4	0.4	0.007	1.4	0.3	0.007
	10	2.6	0.6	0.013	2.5	0.6	0.013	2.5	0.6	0.012
	15	3.7	0.9	0.018	3.6	0.9	0.018	3.6	0.9	0.018

Table C-4. LEO-GEO orbit transfer time

α kg/kWe	S/C P*, W/kg	TSS P*, W/kg	ΣP*, W/kg	v_e, km/s	η	$t_{f(s)}$	t_f, days	X $1.2M
5	200	132	79.4	10	0.5	6.2101×10^5	7.2	8.63
		322	123.4	25	0.5	12.0540	14.0	16.74
		497	142.6	50	0.5	22.2728	25.8	30.93
10	100	77	43.5	10	0.5	11.3363	13.1	15.74
		208	67.6	25	0.5	22.0124	25.5	30.57
		356	78.1	50	0.5	40.6987	47.1	56.53
15	66.7	54	29.9	10	0.5	16.4657	19.1	22.87
		154	46.5	25	0.5	31.9721	37.0	44.41
		275.5	53.7	50	0.5	59.1406	68.45	82.14
5	200	337	125.5	60	0.63	24.3759	28.2	33.86
		450	138.5	80	0.75	25.0875	29.0	34.84
		521	144.5	100	0.785	28.9519	33.5	40.21
10	100	266	72.6	60	0.63	42.1117	48.7	58.49
		368	78.6	80	0.75	44.1817	51.1	61.36
		431	81.2	100	0.785	51.5406	59.7	71.58
15	66.7	219	51.1	60	0.63	59.8559	69.3	83.13
		311	54.9	80	0.75	63.2759	73.2	87.88
		368	56.4	100	0.785	74.1304	85.8	102.96

Table C-5. Self-powered 4-GWe spacecraft transportation cost summary

v_e, km/s	α_{pss}, kg/kWe	Cost, $M					$/kg$_{pss}$
		Hardware	Prop	LEO	Time	Total	
10	5	496	1.2	1519	8.63	2025	1[illegible]
25		325	0.5	621	16.74	963	98
50		284	0.3	404	30.93	719	86
10	10	702	2.1	2598	15.74	3318	133
25		390	0.9	960	30.57	1381	85
50		314	0.6	563	56.53	935	73
10	15	908	3.1	3678	22.87	4612	127
25		454	1.3	1299	44.41	1799	80
50		345	0.9	723	82.14	1151	69
60	5	3244	0.36	593.6	33.86	3872	244
80		2194	0.28	444.1	34.84	2673	184
100		1665	0.25	383.7	40.21	2089	154
60	10	3274	0.62	753.1	58.49	4086	152
80		2213	0.49	543.3	61.36	2818	120
100		1680	0.46	463.5	71.58	2216	105
60	15	3305	0.88	913.0	83.13	4302	122
80		2232	0.71	642.5	87.88	2963	99
100		1696	0.66	543.3	102.96	2342	89

REFERENCES

1. Outlook for Space, Report to NASA Administrators by the Outlook for Space Study Group, NASA SP-386, Washington, D.C., January 1976.

2. A Forecast of Space Technology, 1980-2000, NASA SP-387, Washington, D.C., January 1976.

3. Pawlik, E.V., "Magnetoplasmadynamic Thruster Applications," Proceedings of the Princeton University Conference on Partially Ionized Plasmas, Princeton, N.J., June 10, 11, 12, 1976.

4. Electrical Prototype/Power Processor Unit Final Design Review, Contract NAS3-19730, TRW Systems Group, February 1976.

5. Future Space Transportation Systems Analysis Study, Phase II, Midterm Briefing, Report No. D180-19800-1, Contract NAS9-14323, Boeing Aerospace Company, June 1976.

6. Glaser, P.E., "The Satellite Solar Power Station: An Option for Energy Production on Earth," AIAA Paper No. 75-637, April 1975.

7. Perkins, G.S., "Viking Orbiter 1975 Articulation Control Actuators," Proceedings, 8th Aerospace Mechanisms Symposium, NASA Langley Research Center, October 18-19, 1973.

8. Melbourne, W.E., Interplanetary Trajectories and Payload Capabilities of Advanced Propulsion Vehicles, Technical Report 32-68, Jet Propulsion Laboratory, Pasadena, Calif., March 31, 1961.